Preparation and Properties of Extruded Thermoplastic Starch/Polymer blends

Michel A. Huneault,[1] Hongbo Li[2]

[1]*Chemical and Biotechnological Engineering Department, Université de Sherbrooke, Sherbrooke, QC, Canada J1K 2R1*
[2]*Industrial Materials Institute, National Research Council of Canada, Boucherville, QC, Canada J4B 6Y4*

Received 1 September 2011; accepted 5 January 2012
DOI 10.1002/app.36724
Published online in Wiley Online Library (wileyonlinelibrary.com).

ABSTRACT: This article examines the starch gelatinization and the blend morphology development in blends of thermoplastic starch (TPS) with high-density polyethylene, polypropylene, polystyrene, poly(lactic acid), and polycaprolactone. The TPS gelatinization and mixing with the second polymer was carried out on a twin-screw extrusion process, where the starch was sequentially gelatinized, devolatilized, and then mixed in the molten state with a synthetic polymer. The role of excess water and process temperature on starch gelatinization was assessed by measuring the X-ray scattering. All prepared blends included 25 % TPS that was dispersed in the synthetic polymer matrix. Compatibilized versions of these same blends were obtained by partially substituting the polymer matrices with maleated analogs. The blend morphology was probed by scanning electron microscopy. Complete starch gelatinization was obtained when the gelatinization process was carried out over 100°C regardless of amount of water used as co-plasticizer. The blend morphologies were greatly improved when a maleated compatibilizer was added. Only TPS/PCL blends exhibited a finely dispersed TPS phase without the use of a compatibilizer. In general, the addition of the TPS reduced slightly the tensile modulus and strength of the different polymers and more importantly the elongation at break. J Appl Polym Sci 000: 000–000, 2012

Key words: thermoplastic starch; polymer blends; polysaccharides; renewable resources; plastics

INTRODUCTION

There is currently a strong interest for bio-based and/or biodegradable polymers. The reasons for this interest are varied. On one hand, biomass is expected to become a less expensive source of organic carbon in comparison to fossil feedstock. On the other hand, the biodegradability is attractive in specific applications, where biodegradation can be used as part of a composting scheme to better manage waste or in certain case to limit the inconvenience caused by improper disposal into the environment. Among the bio-based biodegradable material, thermoplastic starch (TPS) is a promising material. Starch is a mixture of two polysaccharides, amylose and amylopectine, that can be obtained from various crops such as corn, wheat, potatoes, peas, cassava, etc. The amylose:amylopectine ratio changes from crop to crop. An increase in amylose content generally results in higher viscosity and more elastic flow behavior in the melt state.[1] It will also enhance mechanical properties of the TPS but this effect will be greatly diminished in highly plasticized starches.[2] Thus, the selection of the starch source and of the plasticizer can be tuned for different applications depending on process or property requirements.

The so-called TPS is produced by mixing the native starch with a plasticizer at a temperature above the starch gelatinization temperature, typically in the 70–90°C range. This operation weakens the hydrogen-bonds present and breaks up the crystalline order in the native starch leading to a fully amorphous free-flowing material. The resulting material is known as plasticized starch, destructured starch, or TPS. The properties and rheology of TPS have been thoroughly investigated.[3–6] As such, the TPS is not a suitable material for most common uses. It is very hygroscopic and its properties and dimensional stability are strongly affected by the humidity level since water is a plasticizer for TPS. In addition, in presence of humidity, the amorphous TPS tends to reform its hydrogen bonds leading to recrystallization (also called retrogradation) and in turn to embrittlement of the material.[7,8] This strong property dependence on plasticizer content can become an advantage, however, when the TPS is blended with another hydrophobic polymer. In this case, the hydrophobic polymer can protect the TPS from direct water contact and moisture uptake while the plasticizer level in the TPS can be used to tune the mechanical properties of the TPS. Therefore, the vast majority of work involving the use of starch as

Correspondence to: M. A. Huneault (michel.huneault@usherbrooke.ca).

a material has focused on blending of TPS and other synthetic polymers.[9–12] The synthetic material can be biodegradable to produce a fully compostable material or can be nonbiodegradable to produce materials for long-term applications.[12] Examples of biodegradable blends include blends of TPS with polycaprolactone,[13] polyester amide,[14] and poly (butylene adipate-*co*-terephthalate),[15] which are petrochemical-based polymers. With the recent commercial introduction of PLA, there has also been a high interest for PLA/TPS blends and these have been investigated in terms of their compatibility[16] and of their processing into injection-molded product, biaxially oriented films,[17] and low-density foams.[18]

The development of polymer-blend morphology during mixing has been reviewed extensively elsewhere.[19–21] It is useful, however to recall some of the governing principles to place into context the TPS/polymer blending operation. The fundamental understanding in this area was developed by investigating the deformation of a single Newtonian droplet subjected to pure shear and elongational flows. It was shown that the deformation is governed by the "capillary number," a dimensionless ratio between viscous forces and interfacial forces. Continuous drop deformation (i.e., leading eventually to breakup) occurs when the capillary number is over a critical value, Ca_{cr}. In pure shear, the critical capillary number shows a minimum for $\lambda = 1$ and increases rapidly with increasing viscosity ratios while in elongational flow, it is relatively independent of the viscosity ratio. Obviously, the flow field in mixing equipment is far more complex and chaotic than in the viscometric experiments. Viscoelastic droplets can also break by different mechanism such as surface erosion[22] and drop splitting.[23,24] Nonetheless, the understanding gained on model Newtonian and non-Newtonian studies has lead to the generally accepted "rules of thumb" that blends with a more viscous dispersed phase and with higher interfacial tension are more difficult to disperse. In particular, large viscosity ratio systems can lead to bimodal size distribution with finely dispersed particles coexisting with some undispersed particles that have not reached that dynamic equilibrium state.[25]

The preparation of TPS/polymer blends boasts the above complexities with the additional feature that the TPS formation itself involves a complex starch destructuration process known as gelatinization. The polymer, starch, and starch plasticizers can be mixed all at once but this was shown to give poorer dispersions than when the gelatinization and the TPS/polymer blending was carried out sequentially in the continuous mixing process.[26] Therefore, a preferred method consists in carrying out the gelatinization in a first stage of the mixing process to form the TPS. Then, the TPS can be mixed with the synthetic polymer to form the immiscible blend structure. Since TPS rheology is very sensitive to plasticization, the blend viscosity ratio can be adjusted by changing the TPS plasticizer level. For glycerol plasticized TPS, for example, the dispersion in PLA, PS, and PE were shown to be particularly coarse until a minimal level of 30 wt% glycerol in the TPS phase was reached.[27–29] Finer morphologies were found past this plasticizer concentration threshold with only a slight dependency on further increase plasticizer addition. This shows the importance of a minimal-TPS plasticization level in the overall blend morphology development. The high interfacial tension between TPS and common synthetic polymers is another factor that can be detrimental to a fine dispersion. Initial reports on PLA/TPS blends, for example, showed extremely coarse morphologies and pinpointed the need for interfacial modification.[30] In situ interfacial reactions between polymers comprising maleic anhydride moieties and TPS have since then been successfully used to reduce interfacial tension in the melt state and improve adhesion in the solid state.[27,31]

Surprisingly, very few scientific publications have systematically investigated the structure development in TPS/polymer blend prepared by a melt-mixing technology. This article examines the structure and property development for different TPS/polymer blends obtained by twin-screw compounding. The investigation examines the moisture content, dispersion, and mechanical properties of compatibilized and uncompatibilized blends of TPS with high-density polyethylene (PE), polypropylene (PP), polystyrene (PS), polylactic acid (PLA), and polycaprolactone (PCL). The compatibilizers were maleated analogs of the different synthetic polymers. The TPS degree of gelatinization was evaluated using X-ray diffraction (XRD), while the blend morphology was observed using scanning electron microscopy (SEM).

EXPERIMENTAL

Materials

Wheat starch was used as the sole-starch source. The starch was an industrial purpose starch grade, Supergel 1201, supplied by ADM. Water and glycerol were used as plasticizers. The glycerol was a 99.5 % pure USP grade supplied by Mat Laboratories.

The grade names and suppliers of PE, PP, PS, PCL, and PLA are summarized in Table I. The blend composition was set to 25 % TPS for all TPS/polymer blends. For compatibilization of the TPS/Polymer blends, functional polymers containing maleic anhydride were used to react with the starch macromolecules to create graft block copolymers that are known to act as emulsifiers in polymer blends. In

TABLE I
List of Polymers with their Grade Names and Suppliers

Name and abbreviation		Grade/supplier	Melt index (g/10 min)
High-density polyethylene	PE	DMDA8920, Petromont	20
Polypropylene copolymer	PP	Profax SB821, Basell	12
Polystyrene	PS	PS 3500, Nova Chemicals	16
Polycaprolactone	PCL	Tone 787 – Dow Chemicals	–
Poly(lactic acid)	PLA	PLA 4032D, Nature Works	–
Maleic anhydride grafted PE	PE-*g*-MAh	Polybond 3009	
Maleic anhydride grafted PP	PP-*g*-MAh	Polybond 3150	
Maleic anhydride grafted PLA	PLA-*g*-MAh	Experimental	
Styrene–maleic anydride copolymer	SMA	Dylark 232, Nova Chemicals	

the case of PE and PP, the functional version were maleic anhydride grafted PE and PP (PE-*g*-MA and PP-*g*-MA). For blends of TPS with PS, a random copolymer of styrene and maleic anhydride, SMA was used. SMA and maleated olefins are known to react with starch and modify the starch–polymer interface.[32] These three maleated polymers are commercially available and the grade names and suppliers can also be found in Table I. For PLA, no such MA-grafted version was commercially available. Thus, PLA-*g*-MA was produced by extruding PLA in presence of 2 % maleic anhydride and 0.25 % organic peroxide. According to the published reports, the grafting level using this technique is around 0.5 %.[33] The unreacted maleic anhydride was removed by vacuum devolatilization. The organic peroxide was Luperox 101. It was adsorbed on a silica support at an effective content of 45 % to facilitate its handling. Both the maleic anhydride and the peroxide were obtained from Aldrich Chemical Company. In compatibilized blends using PE, PP, and PS, 10 % of the polymer was substituted by the maleated analogs. For PLA, 20 % substitution was used.

The interfacial tension between TPS and the different polymer matrices used in this study is an important parameter, since strong interfacial forces will tend to hinder dispersion. Unfortunately, the direct measurement of the interfacial tension between TPS and synthetic materials is difficult since the most common methods such as the "breaking thread" or "drop retraction" methods require the accurate measurement of the Newtonian Plateau viscosity. TPS does not exhibit such a plateau. Therefore, these techniques cannot be used for the investigated polymer pairs. It is possible, however, to get a theoretical estimation of the interfacial tension from the surface tension of pure materials based on the harmonic mean equation[34]:

$$\gamma_{12} = \gamma_1 + \gamma_2 - \frac{4\gamma_1^d\gamma_2^d}{\gamma_1^d + \gamma_2^d} - \frac{4\gamma_1^p\gamma_2^p}{\gamma_1^p + \gamma_2^p} \quad (1)$$

where γ_{12} is the interfacial tension between component 1 and 2, γ_1 and γ_2 are the surface tension of the individual components, while the d and p superscripts refer to dispersive and polar contributions to the surface tension (recognizing than $\gamma_i = \gamma_i^p + \gamma_i^d$) of each material. The dispersive and polar contributions of the different materials at 25°C have been reported in the literature[10,34] and are summarized in Table II along with the interfacial tension between TPS and the different synthetic polymers calculated using eq. (1). The interfacial tension between TPS and PS, PLA and PCL vary only between 5.9 and 7.3 mJ/m^2, while with the nonpolar PP and PE, the values are in a much larger range from 14 to 16.4 mJ/m^2. From an interfacial point of view, the authors therefore have two distinct families of polymer pairs with either intermediate or high interfacial tensions.

Blend rheology

The viscosity of pure materials at 180°C was measured using two methods. For all synthetic polymers, the viscosity was obtained from oscillatory shear experiments performed with a shear amplitude of 10 % using 25 mm plates. In the case of PS, PLA, and PCL, the samples were dried overnight in a vacuum-oven prior to measurement. For the TPS, it was not possible to get a stable response under oscillatory shear because the plasticizer tends to evaporate over the course of the measurement. Therefore, the viscosity measurements were made by capillary rheometry, where the pressurized environment enables plasticizer retention.

TABLE II
Surface Tension Contributions and Calculated Interfacial Tension $\gamma_{TPS/Polymer}$ Between TPS and Selected Polymers

Material and reference	γ (mJ m^{-2})	γ^d (mJ m^{-2})	γ^p (mJ m^{-2})	$\gamma_{TPS/Polymer}$ (mJ m^{-2})
TPS[10]	32	20	12	–
Polystyrene[34]	40.7	34.5	6.1	5.9
PLA[10]	49	37	11	6.1
PCL[10]	52	41	11	7.3
PP[34]	30.1	30.1	0	14
PE[34]	35.7	35.7	0	16.4

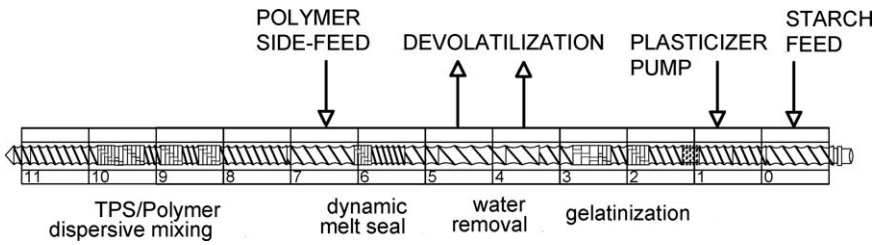

Figure 1 Process configuration for TPS/Polymer blending.

Blend preparation

The TPS/polymer blends were prepared on a Leistritz 34 mm co-rotating twin-screw extruder with an L/D ratio of 42. The process and screw configuration for TPS/polymer blending are presented in Figure 1. The extruder is composed of 12 barrel sections numbered 0 to 11 for reference. The starch was introduced either in a dry-powder form in the feed hopper or in the form of a starch–water–glycerol slurry. When feeding the starch in dry form, the glycerol and water were pumped into the extruder at barrel section 1. A 1 : 10 water : glycerol ratio was used as a standard condition, but this ratio was varied in specific experiments to assess the effect of water on the TPS gelatinization. For slurry incorporation, the composition was adjusted to get a 50 % solid content. The water and glycerol ratio were adjusted to get a final glycerol content of 36 % in the TPS on a water-free basis. An initial humidity content of 9 % in the native starch was assumed for all mixtures. This led to typical slurry comprising 50 wt% starch, 25 wt% water, and 25 wt% glycerol. The slurry was pumped directly into the extruder removing the need for independant plasticizer pumping at barrel section 1. Following starch and plasticizer incorporation, section 2 and 3 of the twin-screw extrusion line were used to gelatinize the starch. Sections 4–6 were used for water removal by devolatilization under vacuum. It has been verified by condensing and analyzing the removed volatiles that glycerol losses in this step were not significant. This first half of the extrusion process was typically operated at $T_{gel} = 140°C$, but for selected experiments, it was decreased down to 85°C to investigate the effect of temperature on the starch gelatinization. The second polymer phase was fed in solid-pellet form to the twin-screw process at barrel section 7 using a conventional side-feeder. Sections 8–11 were used to thoroughly mix the TPS with the second polymer phase and pump the mixture out of the extrusion die. Barrel sections 7–11 were maintained at 180°C in all cases to enable complete melting/softening of the synthetic polymer phase. This sequence of twin-screw operations was successfully used for polyurethane/TPS blends,[35] for polyethylene/TPS blends,[29] and later on biodegradable blends.[36] In the cited published reports, the starch was introduced as a slurry and the second polymer phase was added in molten form using a single-screw extruder as a side-feeder. In the current study, the starch was fed either in dry-powder form or in slurry form, while the polymer was always fed in solid-pellet form.

All blend compounding runs were carried out at a rate of 10 kg/h and strands were extruded through a two-strand die. The strands were air-cooled and pelletized. The PLA was dried prior to compounding and the compounded pellets were dried again in a desiccating dryer at 55°C prior to injection molding.

Pure TPS preparation

In addition to mixing, the twin-screw compounding line was used to extrude pure TPS band as reference materials. The purpose was to produce pure TPS in conditions similar to those existing in the gelatinization portion of the compounding process. The TPS was therefore produced using a shorter screw configuration comprising only barrel Sections 0–7 (see Fig. 1) corresponding to a L/D ratio of 28. A slit die (30 mm × 1 mm) was mounted at the end of the extruder to produce rectangular TPS bands. The bands were supported on a conveyer belt after die exit and air-cooled over a conveyer length of 5 m before being collected. Dry-starch and starch-slurry incorporation methods were used for comparison purposes.

Characterization

Gelatinization

Wide-angle X-ray diffraction measurements were carried out directly on the pure TPS bands. The diffraction patterns were obtained with a D-8 X-Ray Diffractometer (Bruker). The samples were exposed to X-ray beam with the X-ray generators running at 40 kV and 40 mA. The scanning was carried out at a rate of 0.03°/s in the angular region (2θ) of 2–40°.

Blend morphology

The blend morphology was assessed by observation of microtomed surfaces using SEM. The surfaces were prepared using an ultramicrotome at −100°C

using a diamond knife. The surfaces were subsequently treated with hydrochloric acid (HCl, 6N) for 3 h to selectively extract the TPS phase.

Tensile mechanical properties

The TPS/polymer pellets were injection molded into the ASTM D638 standard type I dogbone-shaped samples. Tensile testing was carried out at room temperature using an extension rate of 5 mm/min. A contacting extensometer was used in all cases for precise initial strain measurements. The injected blend samples were tested in the dry as molded state. Pure TPS bands were also tested after extrusion and in some cases (mentioned in text) after conditioning at 25°C and 50 % relative humidity using a controlled temperature and humidity chamber. The dogbone-shaped specimens were punched out of the TPS bands in the machine direction. The thickness of the bands was measured for each test to insure that accurate dimensions were used for stress calculations.

Moisture content

The moisture content of the TPS at extruder exit was evaluated using a weight-loss method. The weight loss was monitored after drying at atmospheric pressure in a desiccating dryer at 105° for seven consecutive days. This method was preferred over Thermogravimetric Analysis because it was simpler and enabled the testing of several samples in the same environment. The use of atmospheric pressure for the drying was essential to prevent glycerol losses that would add to the apparent humidity level of the samples.

RESULTS AND DISCUSSION

Material viscosity

The materials viscosity is an important polymer processing information. Figure 2 presents the viscosity of all materials at 180°C as a function of oscillation frequency (for synthetic polymers) or shear rate (for TPS). The synthetic polymers exhibited to various degrees the typical Newtonian plateau at low frequency followed by a shear-thinning behavior. The TPS did not exhibit any viscosity plateau at low shear rate, behaving as a suspension or partially structured melt, as was reported early in the development of TPS-based materials.[37,38] The material's zero-shear plateau viscosity are ranked in the following order PE < PP < PCL < PLA < PS. The TPS viscosity is intermediate in the investigated materials. The large variation in viscosity may appear detrimental for the purpose of this article since the viscosity ratio between the dispersed phase and the matrix has been shown to play an important role in determining the critical Capillary number (i.e., ratio of shear to interfacial forces) required to deform and break droplets in viscometric flows.[24] As we will discuss later, many other parameters are important in the complex dispersion process and the ability to process and injection-mold the materials was prioritized over attempting to match the viscosity at an arbitrarily selected shear rate-temperature combination.

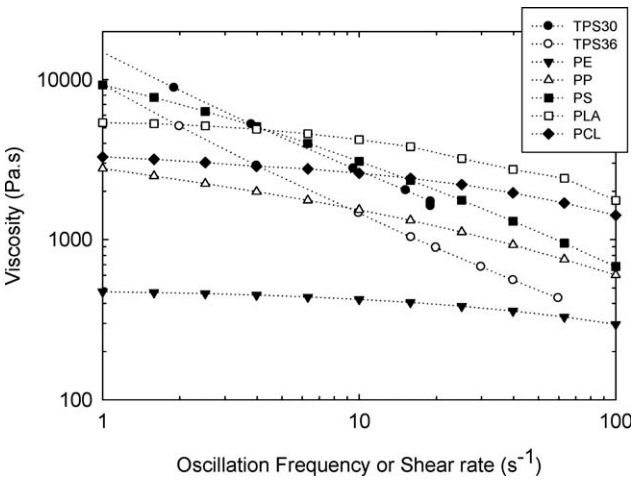

Figure 2 Viscosity of the different materials at 180°C. For the synthetic polymers, the viscosity was measured in oscillatory shear while the TPS viscosity is measured by capillary rheometry.

Starch gelatinization

X-ray diffraction was used to detect changes in the crystalline and ordered structures of starch upon processing and as a way to insure that complete gelatinization was achieved at the end of the compounding process. Native starch is known to have two distinct crystalline forms known as the A-type and B-type. The A-type is present in cereals, while the B-type occurs in tubers. Both involve the hexagonal arrangement of double helices but the structures differ in packing density. By definition, these ordered structures must be destroyed in the gelatinization process.[39] The typical A-type structures present in native starch lead to diffraction peaks at 15.0°, 18.1°, and 22.9°. Once the starch is gelatinized, the linear amylose chains are freed from the starch granules and become fully amorphous. However, if alcohols, fatty acids, monoglycerides, or lipids are present, a new structure may be formed by the complexing of these compounds with amylose. These structures are known as the V-type.[40] It was reported in glycerol-plasticized TPS that X-ray diffraction peaks associated to V-type structures were present at 13.5°, 19.4°, and 20.8°. In addition upon aging of the water-plasticized TPS, B-type structures can be formed leading to peaks at $2\theta = 22.3°$ and 26.1°, a phenomena associated to retrogradation. However, these structures do not form readily in highly plasticized glycerol–TPS.[41]

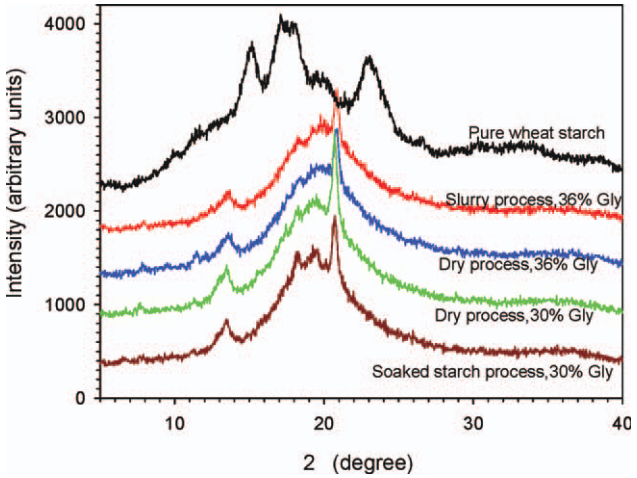

Figure 3 X-ray diffraction intensity scans for pure wheat starch and TPS obtained with the three process variants using a process temperature of 130°C. [Color figure can be viewed in the online issue, which is available at wileyonlinelibrary.com.]

Figure 3 presents XRD diffraction intensity as a function of angle 2θ for TPS obtained with various initial water levels. For practical purposes, the water:glycerol ratio reported in this article refers to the water added along with the glycerol as a co-plasticizer. Later, this water is to a large extent removed by the devolatilization step and thus the XRD measurement were made on sample that had essentially the same water content. The pure wheat starch diffraction scans are presented as reference. The starch peaks are around 15°, 18°, and 23°. These A-type peaks disappeared completely in the TPS processed with various initial water:glycerol ratios. This confirmed that the starch gelatinization was completed in the process prior to the mixing of the TPS with the synthetic polymer regardless of the water content used to accelerate the gelatinization process. Sharp new peaks at 13.5° and 21° and a broader one around 19° have appeared indicative of the development of a V-type structures. Surprisingly, the initial water:glycerol ratio did not have much effect on the diffraction intensity patterns. The use of a high-water content was not necessary to obtain full gelatinization in the extrusion process. Thus, addition of water may be useful for the control of the TPS viscosity but is not strictly necessary for the disruption of the starch crystalline structure.

The second investigated effect was that of the process temperature. In the current setup, the process temperature had to be selected to maximize the water devolatilization rate without causing glycerol losses during devolatilization and without causing thermal degradation of starch. In the current experiment, a (added) water:glycerol ratio of 1 : 10 was used. When including the water already present as moisture in the starch, the initial water level was estimated to be 8 %. Figure 4 presents the effect of the process temperature on the XRD intensity of a TPS containing 36 % of glycerol on a water-free basis. For the TPS produced between 100 and 140°C, the sharp new peaks at 13.5° and 21° and a broader one around 19° have appeared indicative of the development of a V-type structures. At the lower extrusion temperature however, none of these characteristic peaks appeared. The chain-mobility is possibly not sufficient to enable complex formation and no V-type peaks appeared. This is in agreement with earlier finding obtained in solution that showed that amylose complexation requires a minimal temperature to occur.[40]

In Figure 5, we compare the diffraction intensity for native and thermoplastic starch obtained when adding the starch either in the form of slurry and as dry-starch (see Blend preparation in Experimental Section). In both cases, the process was operated at 130 °C. The native starch peaks observed at 15, 18.1 and 22.9° have totally disappeared in all gelatinized starches regardless of the preparation technique. Sharp new peaks at 13.5° and 21° and a broader one around 19° have appeared for the gelatinized starches indicative of the V-type structure. Thus, regardless of the starch introduction method, the gelatinization was completed at the point where the TPS is mixed with the second polymer at mid-extruder. For reference, a blend where the starch was soaked with 30% glycerol 24h prior to extrusion is also shown on the Figure. Soaking the starch with glycerol also enabled the full gelatinization

Final moisture content

The effect of the initial water:glycerol ratio in plasticizer feed on final moisture content was investigated. The final moisture level is important in

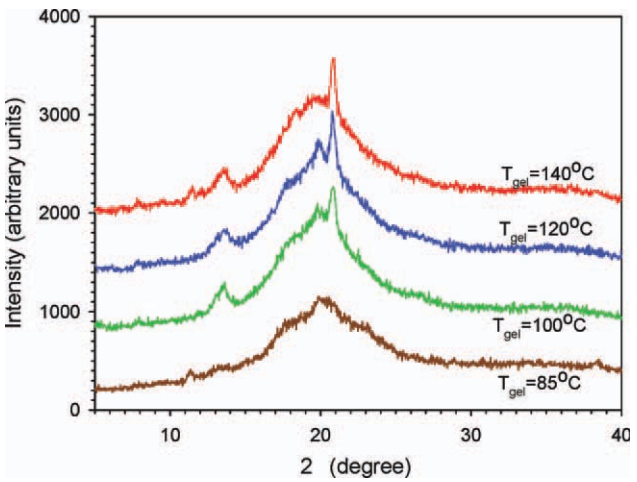

Figure 4 X-ray diffraction intensity for TPS obtained at different process temperatures for a glycerol water ratio of 1 : 10. [Color figure can be viewed in the online issue, which is available at wileyonlinelibrary.com.]

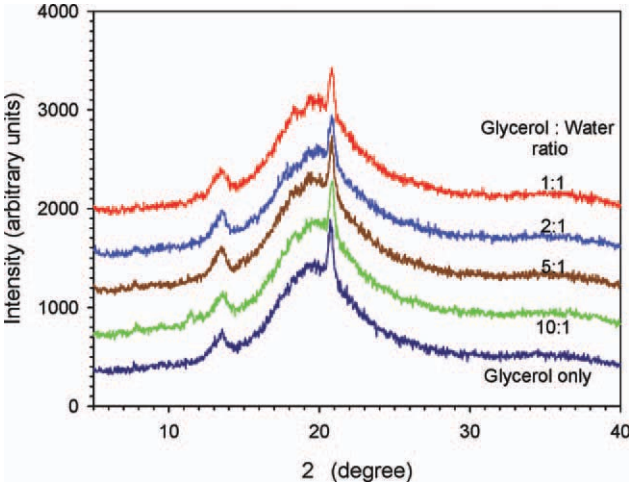

Figure 5 X-ray diffraction intensity for TPS obtained with different glycerol to water ratios using a process temperature of 140°C. [Color figure can be viewed in the online issue, which is available at wileyonlinelibrary.com.]

industrial uses since in many instances, a water-free material will be preferred. In addition, if the TPS is blended with a second polymer phase that is sensitive to hydrolytic degradation, the presence of a high-water content, especially unbound water, may cause chain scission. The glycerol content in the TPS on a water-free basis was maintained in all cases to 36 %. It was the initial water input rate that was varied. Table III presents the initial and final (i.e., after the devolatilization portion of the extrusion process) water level in various TPS. When taking into account, the water already present as moisture in the granular starch, the initial water content varied from 29 % for an initial water:glycerol ratio of 1 : 1 to around 6 % when no additional water was pumped in the extruder. Regardless of these important changes in initial water content, the final moisture level after devolatilization did not vary widely and was much lower than in the equilibrated native starch (i.e., 9 %). At the standard TPS preparation temperature of 140°C, the residual humidity was in the 2–3 % range for the slurry and dry-starch processes. This range is believed to be within normal reproducibility considering the potential variation on the devolatilization efficiency and on the actual polymer temperature in the extruder. Another interesting effect was that of the process temperature. Similar moisture levels were observed when lowering the process temperature to 120°C, but the moisture level increased dramatically when the process temperature was lowered to 100°C and below as the driving force for devolatilization (i.e., water vapor pressure) was lowered.

Dispersion of the TPS phase

The most important measure of mixing quality in a polymer blend is usually the size distribution of the dispersed phase. Figures 6 and 7 present SEM micrographs of uncompatibilized and compatibilized blends obtained with the slurry- and dry-starch incorporation methods. The TPS was selectively removed prior to observation and therefore appears as holes on the micrographs. The compositions are similar in all cases with 25 % TPS in the different continuous phases. The TPS phase comprised 36 % glycerol on a water-free TPS basis. For the slurry process, a 1 : 1 water:glycerol ratio was used in the slurry. Based on the prior results, a 1 : 10 water:glycerol ratio was selected for the dry-starch process. Since water is removed to a great extent in the devolatilization zone of the extrusion process, similar final blend compositions were obtained at the end of the two process variants. The TPS dispersion was coarsest in high-density PE and PP, but the dispersed phase size obtained with the slurry- and dry-starch incorporation methods were similar. The TPS particle diameter in PE ranged between 5 and 15 μm. This is in the same range as those reported earlier for blends with a low-density PE obtained using a starch-slurry incorporation method.[29] In PP, the TPS phases were larger, in excess of 50 μm and

TABLE III
Residual Moisture of TPS Extruded in Various Conditions

Investigated effect	Process	T_{gel} (°C)	Water:glycerol[a] ratio	Initial water content[b]	Final water content (%)
Process effect	Slurry	140	1 : 1	29.4	2.0
	Dry-starch	140	1 : 1	29.4	2.9
$T_{process}$ effect	Dry-starch	120	1 : 10	8.5	2.9
		100	1 : 10	8.5	3.7
		85	1 : 10	8.5	6.6
Glycerol:water ratio effect	Dry-starch	140	1 : 2	19.2	2.9
		140	1 : 5	11.4	2.4
		140	1 : 10	8.5	2.4
		140	Glycerol only	5.4	1.4

[a] Glycerol fraction in on a water-free TPS basis of 30 % instead of 36 for all others.
[b] Accounting for an equilibrium moisture level of 8.9 % in the native starch.

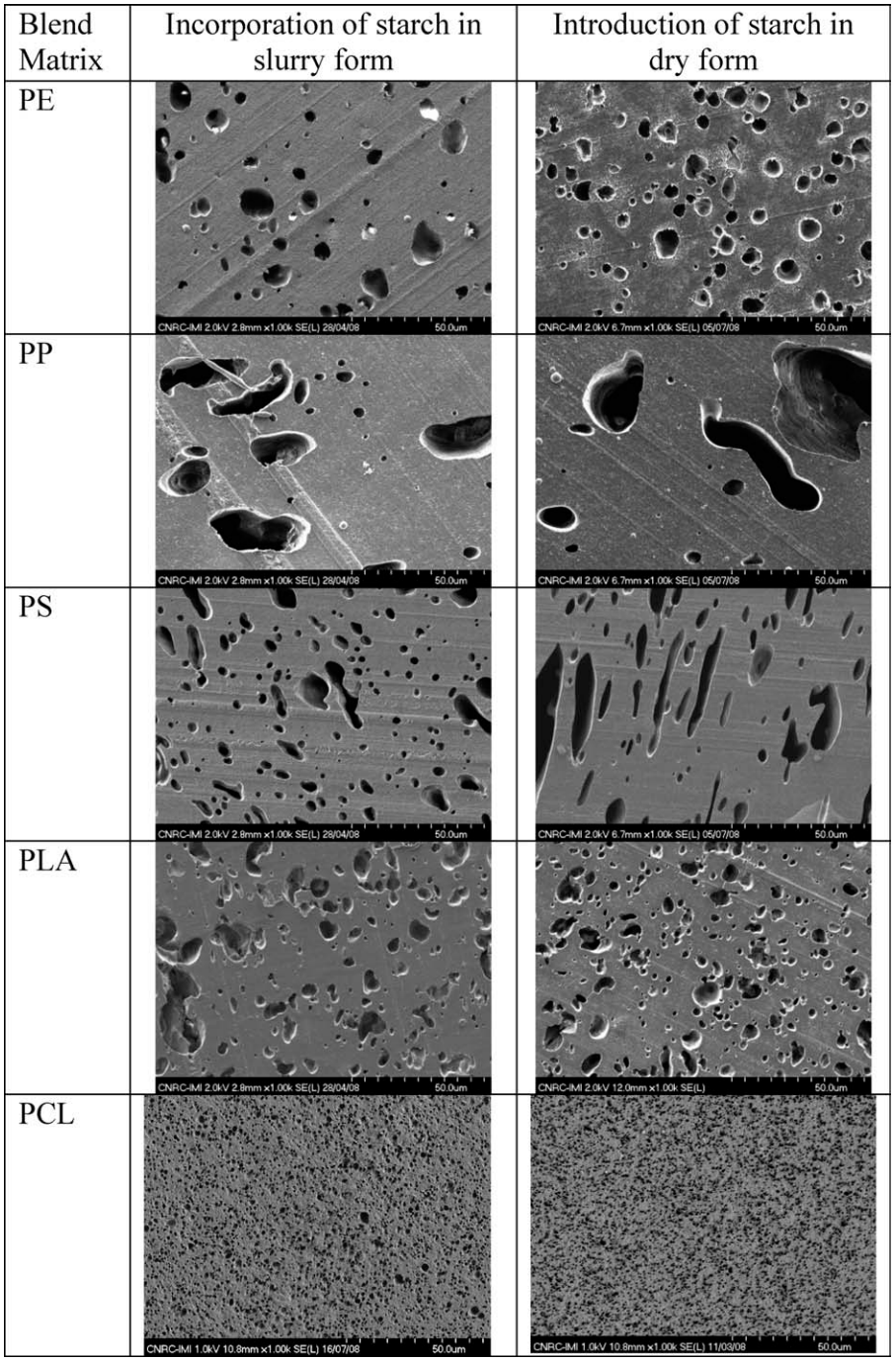

Figure 6 SEM Micrograph of uncompatibilized 25 % TPS/polymer blend produced with the slurry process and the dry-starch process.

with irregular shapes. Obviously, the dispersed phase was capable of coalescing since the final TPS domain size largely exceeded the initial native starch particle dimension (ca. 15–25 μm). In PS and PLA, the TPS particle dimensions were slightly smaller and the particles exhibited more irregular shapes as if they were still in the process of being deformed under flow. The blend morphologies were similar to those reported earlier for PS/TPS and PLA/TPS blends produced using a starch-slurry incorporation method and the addition of the polymer matrices in the melt state.[16,42] Again, no significant morphological differences were observed when comparing the two compounding processes. The last investigated blend was TPS/PCL. For both processes, the morphology was much finer with particle sizes on the micrometer level.

It is interesting to analyze the observed dispersions in relation with our understanding of the rheological and interfacial properties. For the investigated blends, the dispersed phase size ranked into

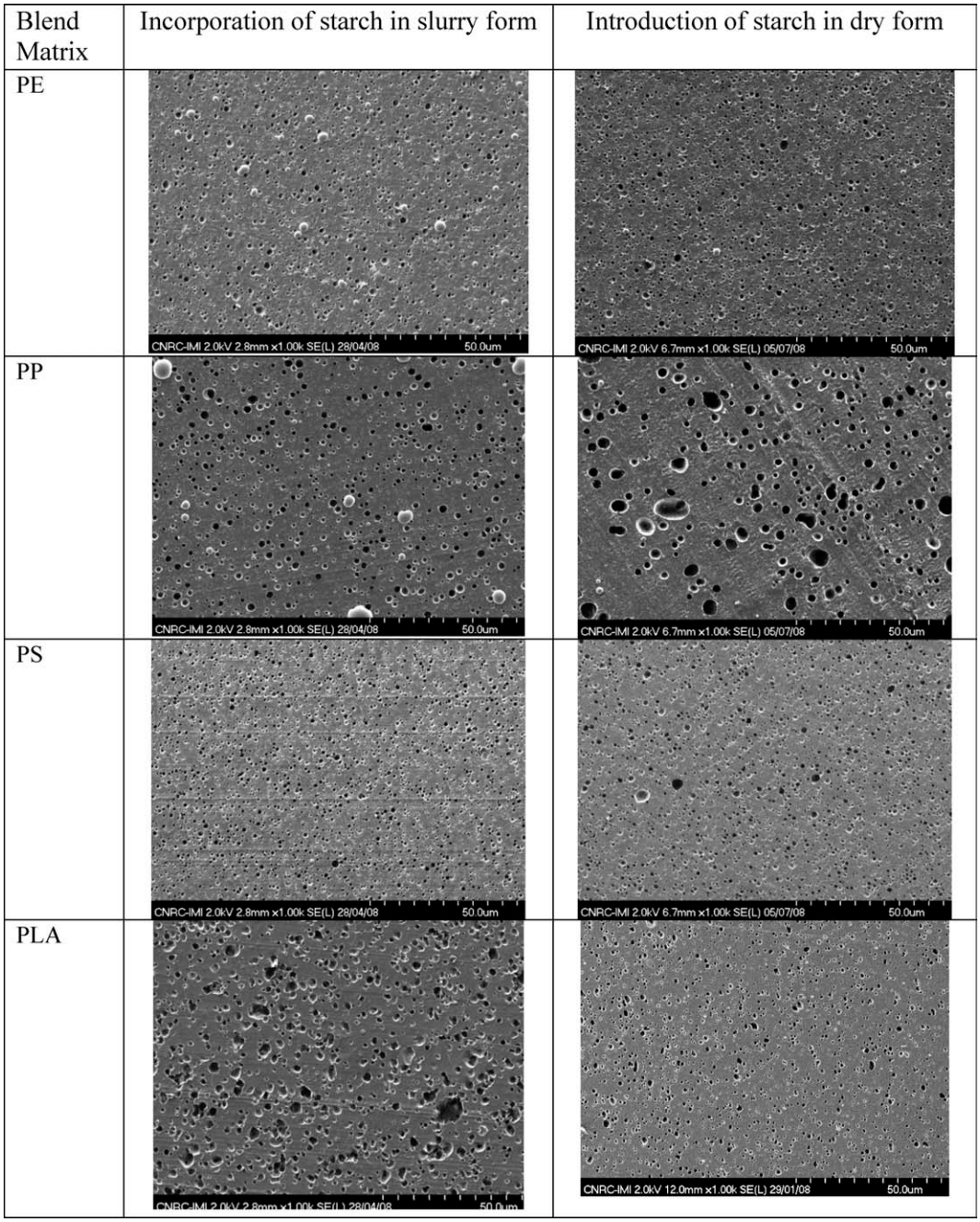

Figure 7 SEM micrograph on 25% TPS/polymer blend compatibilized with maleated polymers produced with the slurry process and the dry-starch process. For PE, PP, and PS, 10% of the polymer was substituted by the maleated analogs. For PLA, 20% substitution was used.

the following order of PCL < PS ≈ PLA < PE < PP. The viscosity ratios, $\lambda = \eta_{dispersed}/\eta_{matrix}$, can be obtained from the viscosity curves in Figure 2. It is noteworthy that the viscosity ratio ranking changed depending on the frequency at which the viscosity curves are compared. At low frequency, the λ ranking was PS < PLA < PCL < PP < PE with the viscosity of the TPS best matched with that of PS. At the highest frequency, the λ ranking became PLA < PCL < PS < PP < PE with the TPS viscosity being better matched with that of PE. If the high frequency comparison is considered more representative, the viscosity ratio was at most around unity (for TPS/PE) and decreased when using the higher viscosity matrices. Therefore, no particular issues related to the high viscosity ratio are expected. At his point, the interfacial tension ranking from Table II should be recalled : PS ≈ PLA < PCL ≪ PP < PE. The TPS/PP and TPS/PE blends fall in a high-interfacial tension range above 14 mJ/m^2, while the three other blends exhibit values in a narrow range between 5.9 and 7.2 mJ/m^2. The significantly higher interfacial

tension of PE and PP and, to a lesser extent, their lower viscosity, can well explain why the TPS/PP and TPS/PE exhibited the coarsest morphologies. The lower interfacial tension of TPS/PS and TPS/PLA blends can also explain their finer morphology. The TPS/PCL system is somewhat odd since it boasts significantly finer particles, while its interfacial tension and viscosity are in the intermediate range. The TPS/PP is also odd, to a lesser extent, since it had to boast a slightly better dispersion than PE based on its lower interfacial tension and lower viscosity ratio. At this point, it may be useful to reflect on the thermal transition of the different polymer matrix. PCL, PE, PP are low glass transition temperature (T_g) materials with a high crystalline content and melting peaks around 60, 127, and 155°C. The PLA grade used in this study is also semi-crystalline with a melting point around 160°C but exhibits much smaller melting enthalpies than PP or PE.[43,44] It also has a much higher T_g, around 57°C, than the previously mentioned polymers. PS is amorphous with glass transitions at 95°C. As explained in the Experimental section, the synthetic polymers were fed in solid form at the middle of the extrusion process, where the TPS was already an amorphous melt flowing at 140°C. Thus, up to the point, where the polymer pellets melt and have sufficiently low viscosity to flow, the liquid TPS minor phase must form the continuous phase of this liquid/solid mixture. Once the synthetic polymer has sufficient fluidity, phase inversion must occur leading to a TPS minor phase dispersed in the major polymer phase. It has been shown that the initial blending stages and the melting order of blend components play an important role in blend morphology evolution. This is especially true, if the minor phase has a lower melting point, thus forcing phase inversion upon melting of the major phase.[20,21] In our case, it may be postulated that the low T_g and low melting temperature of PCL enabled phase inversion at a much lower temperature than with PLA and PS that have high T_g. This changes significantly the stress levels acting on the TPS at the moment of phase inversion. Since it happens sooner in the compounding process, it also leaves a longer residence time to complete the morphological development. Conversely, when comparing PP and PE, the higher melting point of PP may significantly delay the phase inversion in the TPS/PP blend leading to non-equilibrium morphologies at the end of the process. More work on intermediate morphologies would be needed to clarify this mechanism, but it seems that the melting order may explain some of the differences observed between blend systems of similar interfacial tension.

Figure 7 presents SEM micrograph for the same blends as in Figure 6 but in this case in presence of their respective compatibilizing agents described in the Materials section. The compatibilizing agents used in this study are all modified versions of the continuous phase polymer containing various amount of maleic anhydride. The maleic anhydride moieties increase the polarity of the polymer and can potentially react with hydroxyl groups present on the starch macromolecules. This reaction necessarily occurs at the blend interface and thus forms *in situ* graft copolymers that play the role of an emulsifier in the blend. When comparing Figures 6 and 7, it is clear that all the maleated compatibilizers used in the investigation successfully reduced the dispersed phase size. In the PE and PS matrices, the TPS particle size was lowered to the 1–2 μm range. For TPS/PP, the particle size was not decreased to the micron level, but were still significantly reduced when compared with the morphology of the uncompatibilized blends. For the compatibilized TPS/PLA blends, slightly finer morphologies were obtained with the dry-starch process, possibly due to lower residual moisture contents in the TPS since water is known to reduce the reactivity of maleated compatibilizer. The previously reported addition of maleated-LDPE was made by blending together the maleic anhydride and a peroxide initiator[45,46] or by adding maleated PE to the rest of the ingredients without any sequencing of operation. This simultaneous incorporation method lead to much coarser blend morphologies than those presented for PE in Figure 7. This points to the importance of completing the starch gelatinization step before carrying out the TPS/Polymer mixing step in the compounding process. Regarding the PS/TPS compatibilization, the SMA copolymer was extremely effective in reducing the phase size and providing a sharp dispersed phase size distribution. It had been reported that SMA improved tensile properties of Dry-Starch/PS composites[47] but to the authors knowledge, it is the first time that successful TPS/PS blend emulsification is reported. For compatibilized PLA/TPS, the obtained morphologies are similar to those reported earlier with a starch-slurry and molten PLA incorporation method.[16] This confirms that the successful compatibilization results reported earlier are not process-specific.

The reactivity of maleic anhydride moieties is known to be hindered by the presence of water. It was therefore interesting to evaluate the effect of water removal on the obtained morphologies. This variable was explored in the case of TPS/PLA blends. Only the dry-starch incorporation method was used in this study since it seemed to lead to better dispersion results. Figure 8 presents SEM micrographs for three cases. In the first one, no vacuum devolatilization was used (only atmospheric venting) in the extrusion process. In the two other cases, vacuum devolatilization was used but with two

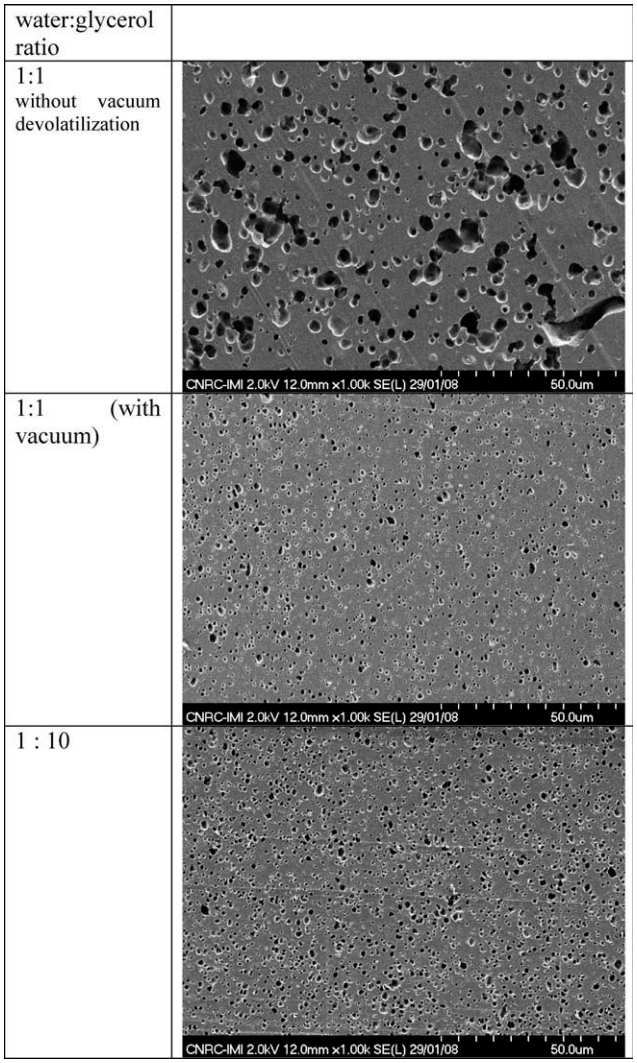

Figure 8 Effect of water:glycerol ratio on morphology of 25% TPS/PLA blends compatibilized with 20% substitution level prepared using dry-starch incorporation method.

different initial water:glycerol ratios. Without the vacuum devolatilization, the blends presented much coarser morphologies as expected from anhydride deactivation. In the two other cases, with widely varying water:glycerol ratios (1 : 10 vs. 1 : 1), very similar final morphologies were obtained. This confirms that the vacuum devolatilization scheme used in this investigation lowered the moisture level to workable levels. It can be envisioned, however that at a larger production scales and at higher throughputs, the devolatilization step may become rate limiting. In that case, the use of the dry-starch incorporation method (rather than the slurry method) and the use of low water:glycerol ratios will become preferable to reduce the required water removal rate.

Tensile mechanical properties

Table IV presents the tensile properties of TPS containing 30–36 % in their "dry as extruded" state. The residual moisture content in the 30, 33, and 36 % glycerol–TPS were 1.6, 2.6, and 2.9 %. The tensile modulus of TPS decreased by a factor of 15, from 3 to 0.2 GPa when the glycerol level was increased from 30 to 36 %. The tensile strength was also dramatically decreased, while the elongation increased from 1 to 200 %. This very rapid transition from a rigid and brittle to a soft and ductile material is typical for plasticized starch. Another important effect is that of humidity pickup after extrusion. The modulus and strength of 36 % glycerol TPS was shown to fall to 5 and 1 MPa, respectively, when saturated to its equilibrium water level. This shows the importance of the continuous polymer phase in controlling the water-uptake of the TPS phase.

The mechanical properties of the TPS/polymer blends will be drastically modified if the TPS phase degrades or if some large undispersed TPS particles are present in the blend. The tensile mechanical properties of TPS and of TPS/polymer blends were therefore measured, in particular, to examine if the different starch incorporation method could lead to significantly different results. Table V presents the tensile properties of the blends containing 25 % TPS in the various investigated polymer matrices. The properties of the pure matrices are given as reference. In the case of PE and PP based blends, the modulus and strength of the blends was similar to that of the PE and PP matrices but the elongation was severely decreased. For the noncompatibilized

TABLE IV
Tensile Properties of Pure TPS at 25°C

Description	Tensile modulus, MPa AVG (STD)	Tensile strength, MPa AVG (STD)	Elongation at break, MPa AVG (STD)
TPS30, as molded[a]	2800 (600)	28 (6)	1 (0.3)
TPS33, as molded[a]	310 (65)	7.7 (0.4)	96 (20)
TPS36, as molded[a]	200 (60)	5.26 (0.3)	198 (80)
TPS36, conditioned to equilibrium humidity[b]	5 (1)	1.0 (0.4)	195 (10)

[a] Dry as molded, measured residual moisture content of 1.6, 2.6, and 2.9 % for TPS30, TPS33, and TPS36 respectively.
[b] Conditioned at 50 % humidity for 7 day, moisture content of 8.8 %.

TABLE V
Tensile Properties of Blends and Compatibilized Blends at 25°C

Materials	Process variant	Modulus (GPa)	Tensile strength (MPa)	Elongation at break (%)
PE		1.12	17.9	>800
TPS/PE	Slurry	1.41	16.0	133
	Dry	1.05	15.8	233
TPS/PE/PE-*g*-MA[a]	Slurry	1.14	18.7	27
	Dry	0.935	16.0	>800
PP		1.00	18.8	700
TPS/PP	Slurry	1.06	16.8	19
	Dry	0.914	16.4	12
TPS/PP/PP-*g*-MA[a]	Slurry	1.16	19.85	15
	Dry	0.989	18.0	44
PS		3.28	37.0	2.0
TPS/PS	Slurry	3.09	34.1	1.9
	Dry	2.97	31.0	2.1
TPS/PS/SMA[a]	Slurry	3.13	31.5	1.4
	Dry	2.87	31.9	2.0
PLA		3.68	69.2	6.0
TPS/PLA	Slurry	3.20	49.0	4.9
	Dry	3.33	46.6	4.0
TPS/PLA/ PLA-*g*-MA[a]	Slurry	3.18	49.6	4.2
	Dry	2.96	45.8	6.8
PCL		0.43	25	>800
TPS/PCL	Slurry	0.339	12.3	>800
	Dry	0.259	11.0	>800

[a] Compatibilized blends.

TPS/PE blends, the elongation obtained with the dry-process was significantly higher when compared with the slurry process. The effect was even more pronounced in the compatibilized TPS/PE and TPS/PP cases. In fact, for the PE-based blend, the samples were able to extend up to the maximum extension of the tensile-testing equipment (i.e., 800 %). PS and PLA are more rigid matrices. The addition of TPS, therefore, decreased the modulus and strength in a more significant way but left nearly unchanged the already low elongation at break of the matrices. The TPS and PCL are known to be more compatible without the use of an interfacial modifier. The tensile modulus and strength were decreased with addition of the TPS phase but the elongation at break remained in excess of 800 %. Overall, relatively similar tensile properties were achieved with the slurry- and dry-starch incorporation methods. The dry-process, however, may have an advantage in blends with water-sensitive materials because of the lower achievable TPS moisture content.

CONCLUSION

This article has investigated the structure development in the starch gelatinization and TPS mixing with PE, PP, PS, PLA, or PCL and has compared two starch/plasticizer incorporation schemes referred to as the starch-slurry and dry-starch methods. The disruption of crystalline order in the native starch, monitored by X-ray diffraction, was obtained regardless of the process when the starch and plasticizers were mixed at temperatures in excess of 85°C.

In terms of blend morphologies, the noncompatibilized TPS/polymer blends exhibited coarse morphologies and these morphologies were relatively similar for the slurry and dry-starch incorporation methods. The use of maleated polymer analogs was very efficient in emulsifying the TPS/polymer blends. Much finer and better distributed dispersed phase were obtained when replacing some of the matrix material by the maleated analogs. The use of a process where the TPS is gelatinized prior to being mixed with the polymer matrix lead to finer morphologies in comparison to one-step incorporation methods previously reported.

The tensile modulus and strength of the blends were decreased by addition of the TPS. Obviously, this effect was most evident in the more rigid materials. Similar blend mechanical properties were obtained using the slurry and dry-starch processes and these two methods enabled fabrication of TPS with high plasticizer contents. The slurry method however required the use of a high initial water fraction to maintain sufficient slurry fluidity. The dry-starch method in which the starch and plasticizer were fed sequentially in the extruder was shown to be more flexible since it enabled the use of any desired plasticizer and initial water level and did not require any premixing step. The lower initial water content that could be used with the dry-starch method decreased the required devolatilization rates without any apparent loss in terms of blends properties.

References

1. Della Valle, G.; Vergnes, B.; Lourdin, D. Int Polym Process 2007, 22, 471.
2. Lourdin, D.; DellaValle, G.; Colonna, P. Carbohydr Polym 1995, 27, 261.
3. Aichholzer, W.; Fritz, H. G. Starch Starke 1998, 50, 77.
4. Vergnes, B.; Villemaire, J. P. Rheol Acta 1987, 26, 570.
5. Villar, M. A.; Thomas, E. L.; Armstrong, R. C. Polymer 1995, 36, 1869.
6. Willett, J. L.; Jasberg, B. K.; Swanson, C. L. Polym Eng Sci 1995, 35, 202.
7. vanSoest, J. J. G.; Hulleman, S. H. D.; deWit, D.; Vliegenthart, J. F. G. Ind Crops Prod 1996, 5, 11.
8. VanSoest, J. J. G.; Knooren, N. J Appl Polym Sci 1997, 64, 1411.
9. Averous, L. J Macromol Sci Polym Rev 2004, C44, 231.
10. Schwach, E.; Averous, L. Polym Int 2004, 53, 2115.
11. Wang, X. L.; Yang, K. K.; Wang, Y. Z. J Macromol Sci Polym Rev 2003, C43, 385.
12. Simmons, S.; Thomas, E. L. J Appl Polym Sci 1995, 58, 2259.
13. Averous, L.; Moro, L.; Dole, P.; Fringant, C. Polymer 2000, 41, 4157.

14. Averous, L.; Fauconnier, N.; Moro, L.; Fringant, C. J Appl Polym Sci 2000, 76, 1117.
15. Raquez, J. M.; Nabar, Y.; Narayan, R.; Dubois, P. Polym Eng Sci 2008, 48, 1747.
16. Huneault, M. A.; Li, H. Polymer 2007, 48, 270.
17. Chapleau, N.; Huneault, M. A.; Li, H. Int Polym Process 2007, 22, 402.
18. Mihai, M.; Huneault, M. A.; Favis, B. D.; Li, H. Macromol Biosci 2007, 7, 907.
19. Huneault, M. A.; Shi, Z. H.; Utracki, L. A. Polym Eng Sci 1995, 35, 115.
20. Scott, C. E.; Macosko, C. W. Polymer 1995, 36, 461.
21. Sundararaj, U.; Macosko, C. W.; Shih, C. K. Polym Eng Sci 1996, 36, 1769.
22. Lin, B.; Sundararaj, U.; Mighri, F.; Huneault, M. A. Polym Eng Sci 2003, 43, 891.
23. Mighri, F.; Huneault, M. A. J Rheol 2001, 45, 783.
24. Mighri, F.; Huneault, M. A. Can J Chem Eng 2002, 80, 1028.
25. Huneault, M. A.; Mighri, F.; Ko, G. H.; Watanabe, F. Polym Eng Sci 2001, 41, 672.
26. Li, H.; Huneault, M. A. J Appl Polym Science 2011,119, 2439.
27. Huneault, M. A.; Li, H. Polymer 2007, 48, 270.
28. Mihai, M.; Huneault, M. A.; Favis, B. D. J Cell Plastics 2007, 43, 215.
29. Rodriguez-Gonzalez, F. J.; Ramsay, B. A.; Favis, B. D. Polymer 2003, 44, 1517.
30. Martin, O.; Averous, L. Polymer 2001, 42, 6209.
31. Dole, P.; Averous, L.; Joly, C.; Della Valle, G.; Bliard, C. Polym Eng Sci 2005, 45, 217.
32. Seethamraju, K.; Bhattacharya, M.; Vaidya, U. R.; Fulcher, R. G. Rheol Acta 1994, 33, 553.
33. Carlson, D.; Nie, L.; Narayan, R.; Dubois, P. J Appl Polym Sci 1999, 72, 477.
34. Wu, S. Polymer Interface and Adhesion; Marcel Dekker: New-York, 1982.
35. Seidenstucker, T.; Fritz, H. G. Starch Starke 1999, 51, 93.
36. Sarazin, P.; Li, G.; Orts, W. J.; Favis, B. D. Polymer 2008, 49, 599.
37. Aichholzer, W.; Fritz, H. G. Starch Starke 1998, 50, 77.
38. Villar, M. A.; Thomas, E. L.; Armstrong, R. C. Polymer 1995, 36, 1869.
39. Cooke, D.; Gidley, M. J. Carbohydr Res 1992, 227, 103.
40. Le Bail, P.; Bizot, H.; Ollivon, M.; Keller, G.; Bourgaux, C.; Buleon, A. Biopolymers 1999, 50, 99.
41. Shi, R.; Liu, Q. Y.; Ding, T.; Han, Y. M.; Zhang, L. Q.; Chen, D. F.; Tian, W. J Appl Polym Sci 2007, 103, 574–586.
42. Mihai, M.; Huneault, M. A.; Favis, B. D. J Cell Plastics 2007, 43, 215.
43. Li, H.; Huneault, M. A. Polymer 2007, 48, 6855.
44. Li, H.; Huneault, M. A. Int Polym Process 2008, 23, 412.
45. Wang, S. J.; Yu, J. G.; Yu, J. L. J Appl Polym Sci 2004, 93, 686.
46. Wang, S. J.; Yu, J. G.; Yu, J. L. Polym Int 2005, 54, 279.
47. Vaidya, U. R.; Bhattacharya, M. J Appl Polym Sci 1994, 52, 617.